Relationship between the receiver diameter and the light flux fluctuations in a narrow divergent laser beam propagating through a snowfall. Part 2. Autocorrelation function

A.F. Zhukov and N.A. Vostretsov

Institute of Atmospheric Optics,
Siberian Branch of the Russian Academy of Sciences, Tomsk

Received June 19, 2000

We have measured autocorrelation function of a narrow divergent laser beam propagated along 10 different paths (from 14 to 1928 m) under snowfall conditions. The correlation time was analyzed at the levels of 0.5, 0.3, 0.1, 0.05, and zero level depending on the receiver's diameter (D_r), wind velocity ($V_\perp$), and maximum size of particles in the snowfall (D_m). It is shown that under close (similar) atmospheric conditions, that is, $V_\perp$ and D_m the correlation time at 0.5 level decreases with the decrease of the receiver's diameter. It also decreases at a fixed D_r with the growth of $V_\perp$ and decreasing D_m.

Introduction

It is known that the atmosphere significantly worsens certain characteristics of a laser beam when the atmospheric precipitation occurs. The beam is attenuated owing to the scattering by particles of atmospheric precipitation and aerosol. Moreover, in addition to turbulent fluctuations of the air refractive index the particles of atmospheric precipitation cause strong fluctuations of received radiation. Thus, a signal at the output of a photodetector can be considered as a random value in time. It is especially clearly in the cases when the sizes of a receiver are smaller or a little bit larger, as compared with the size of particles.

It is naturally that statistical characteristics of such fluctuations differ from the analogous ones in the turbulent atmosphere without atmospheric precipitation. The latter are of interest for a long time and up to now they are well studied.

Normalized autocorrelation function (NACF) is one of the basic statistical characteristics of a random process. It gives a measure of the interrelation between random signals delayed at some interval in time.

In combination with other statistical characteristics, it is used to optimize the reception of radiation propagated through the atmosphere. Peculiarities of NACF in atmospheric precipitation are not studied that well. However we should expect a decrease of the correlation time because the temporal spectrum of fluctuations in atmospheric precipitation spreads noticeably into the range of high frequencies.

The goal of this paper was to study the peculiarities of NACF due to the change of the receiver's diameter D_r. The NACF was measured in a narrow divergent beam (NDB) under snowfall conditions. This paper is a continuation of Ref. 1 where the equipment and measurement technique used were described in detail. For this reason we shall not describe the measurements in detail and focus on the peculiarities of the correlation function.

1. Brief description of the experiment

The autocorrelation functions (ACF) were measured using receivers with different diameters D_r. At $D_r = 0.1$ mm the measurements under snowfall conditions were carried out on the paths 14, 37, 130, 260, 780, 964, and 1928 m long, and for other receiver diameters ($D_r > 0.1$ mm) on the paths of 260, 520, and 780 m lengths.

As a light beam the radiation from LGN–215 and LG–38A lasers was used. The lasers were operated under the quasi-single-mode regime with the linear polarization of radiation. Polarization plane was approximately perpendicular to the Earth's surface. The laser beam without some transformation was directed to the atmosphere. Basic parameters of the beam are: the wavelength $\lambda = 0.6238$ μm; the initial diameter (at the level 1/e) 3–4 mm; the total angle of divergence $5 \cdot 10^{-4}$ rad.

The radiation was received by a photoelectric multiplier (PMT), the diaphragms with the diameter $D_r = 0.1$–25 mm and interference and neutral density filters were placed in front of it. The blind located before the receiver limited the field-of-view angle of the receiver. The total field-of-view angle of the receiver was $2.7 \cdot 10^{-2}$ rad. The signal from the photodetector was amplified and then entered into at an X6–4 correlator, spectrum analyzer FSP–38, pulse analyzer AI–1024, and the variance meter that was developed in accordance with the recommendations in Ref. 2.

Let us present some information on the X6–4 correlator. It is a digital device that simultaneously measures 100 values of a correlation function. Normalization of the ACF was performed to its value at zero delay.

To characterize the NACF, we used its five values equaled to 0.5; 0.367; 0.1; 0.05, and the first value equals to zero. For each value we obtained the corresponding time delay, which we call the correlation time at 0.5; 0.3; 0.1; 0.05, and zero level. Let $t_{0.5}$; $t_{0.3}$;

0235-6880/00/11 962-08 $02.00

$t_{0.1}$; $t_{0.05}$, and t_0 denote the levels. These values of time equally along with the NACF themselves were the subject of our research. Let us emphasize that in accordance with Ref. 3, p. 264, the time $t_{0.05}$ can be taken as a maximum interval of correlation allowing for the conclusions ibidem. The calculated time of the ACF averaging was not less then 4 s. The measurement error in ACF values by our estimations did not exceed 10%. Two hundred NACF values measured in 55 snowfalls were analyzed.

The optical depth of the measurement path τ, maximum size of snowflakes D_m, and wind velocity V and its component $V_\perp$ characterized the atmospheric conditions.

Now few words must be said on the peculiarities of snowfall which are important for measurements.

1. Snowfall as other atmospheric precipitation is a nonstationary natural phenomenon because its intensity and microstructure of particles change during the time. Moreover, they do not depend on the experimenter and, naturally, they can not be predicted in time.

2. Snowfall effects the optical characteristics of the atmospheric turbulence.

Equally with these natural peculiarities, we ought to take into consideration the fact that the set of optically important characteristics of the atmosphere which were measured in the experiment was not complete.

These circumstances in strong measure cause difficulties in choosing similar (close) conditions of experiment, which are necessary for comparing the results obtained.

We have made measurements so that fluctuations of optical radiation during the measurements could be considered steady state ones, although, on the whole it is impossible to consider the process to be stationary. It is rather a quasistationary process during a certain short time. We obtained such periods by a value of averaged signal and its variance along the measurement path. A time constant of RC-filters in measurement channel (average value and variance) equaled to 20 s. The cases of fast change of the foregoing values were excluded from measurements. We considered the changes occurred during the time interval shorter than 20 s as fast changes, and a value of these measurements exceeded 10%. For the same reasons on the paths with reflection (which have the lengths multiple to 130 m) the data on visibility range obtained using an RDV-3 visibility meter.

2. Results of analysis

2.1. Conditions of experiment

In the data under analysis the length L varied from 14 to 2048 m; D_r varied from 0.1 to 25 mm; V varied from 0 to 7 m/s; $V_\perp$ varied from 0 to 5.6 m/s; D_m varied from 1 to 20 mm; τ varied from 0.03 to 3; and S_m varied from 10 to 0.2 km. Under conditions which limits have been determined above the most correlation time at the level 0.5 $t_{0.5}$ = 4.9 ms was obtained for τ = 0.53; D_m = 5–7 mm; D_r = 25 mm; V = 3.5 m/s; and $V_\perp$ = 1.2 m/s at the path 520 m (Fig. 1*b*, the curve *5*). The minimum correlation time $t_{0.5}$ = 0.07 ms was obtained for τ = 0.05; D_m = = 1–2 mm; D_r = 0.1 mm; V = 6 m/s; and $V_\perp$ = 5.6 m/s at the path 37 m (Fig. 3*e*, the curve *1*). Thus the correlation time $t_{0.5}$ in the analyzed data varied from several milliseconds up to several hundredths of a millisecond. Below we will denote NACF as $b(t)$.

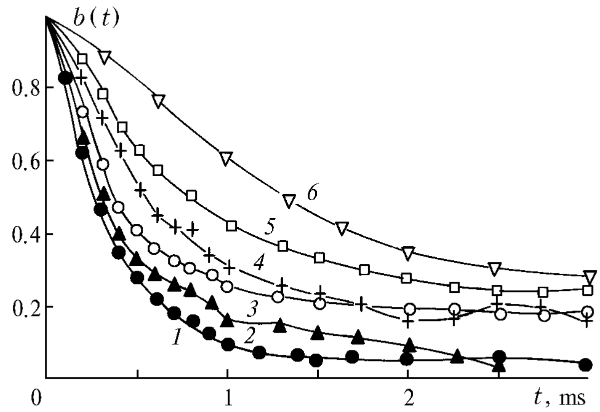

a

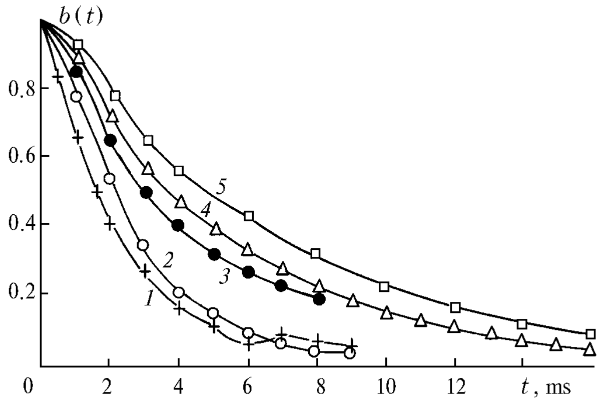

b

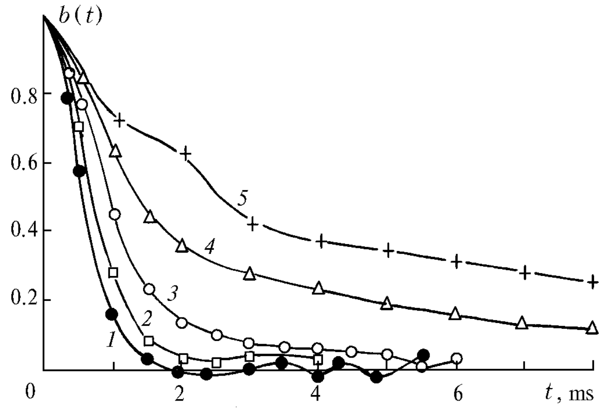

c

Fig. 1.

2.2. Dependence of the NACF on the receiver diameter

Figure 1 presents $b(t)$ for different values of D_r and the path lengths of 260 (*a*), 520 (*b*), and 780 (*c*). We notice that the scale at the horizontal axes in Fig. 1 is different and the growth of $t_{0.5}$ and $t_{0.3}$ is seen clearly with the increase of the receiver's diameter.

The atmospheric conditions during the measurements given in Table 1 varied noticeably for the paths 780 and 520 m and were practically the same for the path of 260 m length. But, in all three cases the correlation time $t_{0.5}$ and $t_{0.3}$ grows with the increase of D_r. This emphasizes the importance of the receiver's diameter.

Figure 2*a* shows the dependence of the logarithm of correlation time on the logarithm of receiver diameter for the path with the length of 520 m, where curve *1* is for $t_{0.5}$; curve *2* is for $t_{0.3}$, and curve *3* is for $t_{0.1}$. The values t_c (and $\log t_c$) are taken from Fig. 1*b*, corresponding meteorological conditions are presented in Table 1. It is characteristic that the dependence of $\log t_c$ on $\log D_r$ has a linear growth. In coordinates $t_c = F(D_r)$ the power-law dependence $t_c = A_0 D_r^{B_0}$ is followed quite closely. For $t_{0.5}$ the values are $A_0 = 2398$; $B_0 = 0.205$, for $t_{0.3}$ the values are $A_0 = 3113$; $B_0 = 0.205$, and for $t_{0.1}$ the values are $A_0 = 6982$; $B_0 = 0.21$ (t_c in ms; D_r in mm).

Figure 2*b* is analogous to Fig. 2*a* but here we show the change of t_c with the growth of D_r for three paths (520 (*1*), 260 (*2*), and 780 m (*3*)) under various meteorological conditions. It is characteristic that a growth is observed of the correlation time ($t_{0.5}$) with the increase of D_r which is close to a linear dependence. It is one of the most important peculiarities of $b(t)$.

Table 1

Date	D_r, mm	L, m	σ^2	τ	D_m, mm	V, m/s		t, ms					Fig.	Curve	$A_{0.5}$
						V	$V_\perp$	0.5	0.3	0.1	0.05	0			
11.06.93	0.1	260	0.08	0.26	1	4.5	1.1	0.272	0.388	0.999	1.665	–	1*a*	*1*	0.43
»	0.8	»	0.07	0.27	1	4	1.4	0.310	0.466	1.655	–	–	»	*2*	0.41
»	1.5	»	0.06	0.27	1	4.5	1.1	0.377	0.610	–	–	–	»	*3*	0.38
»	2.0	»	0.04	0.28	1	4	0.7	0.549	0.822	–	–	–	»	*4*	0.48
»	3.1	»	0.04	0.29	1	4	0.7	0.685	1.332	–	–	–	»	*5*	0.93
»	25	»	0.01	0.30	1	4	0.7	1.332	1.998	–	–	–	»	*6*	0.23
02.20.95	0.1	520	0.38	0.58	3–5 i.f.*	2	0.7	1.660	2.300	5.500	–	–	1*b*	*1*	–
»	0.8	»	0.34	0.58	–	2	–	2.100	2.900	5.999	–	–	»	*2*	–
»	3.1	»	0.28	0.55	3–5 i.f.*	3	–	3.000	4.500	–	–	–	»	*3*	–
»	10	»	0.17	0.44	–	2	–	3.830	5.250	12.00	24.00	55.00	»	*4*	
»	25	»	0.09	0.53	5–7	3.5	1.2	4.900	7.099	15.00	30.00	70.00	»	*5*	0.84
03.10.95	0.1	780	0.74	1.70	1–2	–	–	0.577	0.716	1.260	1.400	1.900	1*c*	*1*	–
»	0.8	»	0.62	1.37	1–3	–	–	0.728	0.864	1.490	1.600	3.500	»	*2*	–
»	3.1	»	0.38	2.63	1–3	0.5	0.2	0.928	1.170	2.600	5.000	–	»	*3*	0.06
»	10	»	0.11	2.22	1–2	0.5	0.2	1.300	1.800	–	–	–	»	*4*	0.13
»	25	»	–	–	1–2	–	–	2.684	4.660	16.00	63.00	80.00	»	*5*	
01.19.94	0.1	260	0.05	0.28	1	1	0.8	0.350	0.530	4.500	–	–	3*a*	*1*	0.28
10.09.93	»	»	0.48	0.45	10	2.5	2.5	0.470	0.760	6.000	–	–	»	*2*	0.12
01.17.94	»	»	0.34	0.51	10	3	0.4	1.025	1.460	4.000	7.000	–	»	*3*	0.04
02.04.94	3.1	»	0.03	0.42	1	2	1	0.560	0.750	1.500	3.500	5.500	3*b*	*1*	0.56
»	»	»	0.39	1	3–5	2	0.8	1.000	1.350	3.500	7.000	–	»	*2*	0.16
»	»	»	0.01	0.18	1–4	1.2	0.7	1.550	1.950	5.000	6.000	8.400	»	*3*	0.27
11.08.94	»	520	0.31	0.98	2	4	1.4	0.400	0.550	2.000	3.500	–	3*c*	*1*	0.28
»	»	»	0.38	1.38	2–5	5	1.7	0.825	1.200	3.900	9.500	–	»	*2*	0.28
»	»	»	0.74	3.04	5–10	3.5	1.9	1.085	1.600	6.000	8.000	–	»	*3*	0.20
11.02.95	25	»	0.01	0.30	1	4	0.7	1.330	1.910	9.930	13.00	19.80	3*d*	*1*	0.93
10.10.95	»	»	0.09	0.74	3–5	2	2	2.000	3.880	8.000	11.00	65.00	»	*2*	0.80
02.20.95	»	»	0.09	0.63	5–7	3.5	1.2	4.600	6.600	16.00	32.00	65.00	»	*3*	0.78
12.14.95	0.1	37	0.02	0.05	1–2	6	5.6	0.07	0.101	0.295	0.365	0.550	3*e*	*1*	0.20
01.24.96	»	»	0.05	0.12	1–2	5	4.3	0.14	0.19	0.53	0.75	–	»	*2*	0.30
12.14. 95	»	»	0.09	0.15	1–3	5	4.3	0.17	0.29	0.60	0.85	–	»	*3*	0.24
11.02.93	»	260	0.03	0.12	1–2	5.5	1.9	0.16	0.26	1.71	–	–	3*f*	*1*	0.15
»	»	»	0.02	0.07	1	2.5	1.25	0.25	0.42	–	–	–	»	*2*	0.31
»	»	»	0.22	0.41	1–2	3.5	0.6	0.41	0.60	1.99	–	–	»	*3*	0.12

* Individual flakes.

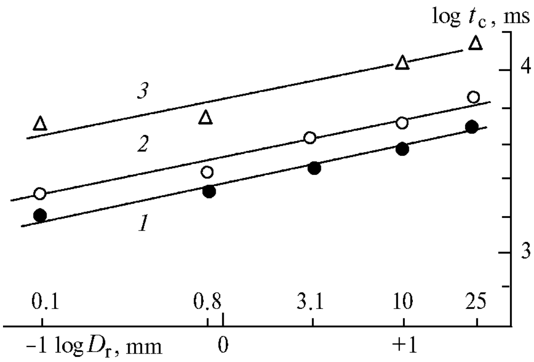

a

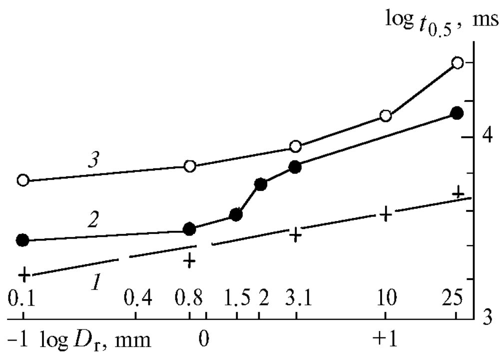

b

Fig. 2.

2.3. Dependence of NACF on wind velocity $V_\perp$ and maximum size of particles D_m

The NACF directly depends on $V_\perp$ and D_m at fixed values of D_r, what we repeatedly observed in the experiments. The dependence of $b(t)$ on D_m is shown in Figs. 3*a*–*e* (additional information is given in Table 1). It follows from these data that the correlation time at the levels 0.5 and 0.3 decreases essentially with the decrease of maximum size of snowflakes (D_m) at close values of the wind velocity ($V_\perp$). We have already discussed this in Ref. 4, p. 133, where the table and plots of $b(t)$ measured on one path with the length of 260 m are presented.

On the other hand, the correlation decreases with the growth of $V_\perp$ and this peculiarity occurs for other paths and receivers (Figs. 3*e* and *f*).

In contrast to $b(t)$ the averaged level of fluctuations $\bar{\sigma}_I$ according to our data does not depend on the wind velocity V and $V_\perp$ (Fig. 4 where the measurement results from Ref. 5 are presented).

The dependence of the level of fluctuations on D_m, which was considered earlier and the practically neutral dependence $\bar{\sigma}_I$ on the wind velocity V and its $V_\perp$ are well seen in Fig. 4 (curve *1* is for $D_m > 5$ mm, $\tau = 2.3$–2.4; curve *2* is for $D_m > 5$ mm, $\tau = 0.5$–0.6; and curve *3* is for $D_m = 1$ mm, $\tau = 0.7$–0.8).

We can suppose from the previous discussion that for the correlation time at the level 0.5 the following relation is correct:

$$t_{0.5} = A_{0.5}\,(D_m/V_\perp)$$

where $A_{0.5}$ is the dimensionless unknown coefficient to be determined:

$$A_{0.5} = (t_{0.5}\,V_\perp)/D_m.$$

What one can expect in the change of $A_{0.5}$?

1. Coefficient $A_{0.5}$ will increase with the growth of the receiver diameter, since for equal relation $V_\perp/D_m$ the correlation time increases (for equal or close values of τ) with the growth of D_r.

2. Coefficient $A_{0.5}$ must not depend on the $V_\perp/D_m$ ratio at a fixed D_r and close values of τ.

3. For essentially different τ the coefficient $A_{0.5}$ must decrease at the large τ because the spatial radius of the intensity correlation decreases.[16] D_r is constant in this case.

4. We assume that the peculiarities pointed out in points 1–3 must reveal themselves regularly when the wind velocity $V_\perp$ exceeds the velocity of the gravitational fall of snowflake and for the measurements of average (possibly, and the most probable) dimension of snowflakes.

In the absence of such information, the peculiarities in $A_{0.5}$ pointed out above cannot manifest themselves at all or are revealed as a random tendency.

As an example in Table 2 we present the average values of $A_{0.5}$ for four D_r values and show the minimum and maximum values of $A_{0.5}$, and also a number N of $A_{0.5}$ used in calculating its average value.

Table 2

D_r, mm	$\bar{A}_{0.5}$	N	$A_{0.5}^{min}$	$A_{0.5}^{max}$
2.5	1.52	10	0.16	3.78
3.1	0.48	28	0.06	1.95
0.8	0.309	33	0.08	0.68
0.1	0.266	72	0.01	0.99

Figure 5 presents the values of $A_{0.5}$ for the receiver with $D_r = 0.1$ mm for the path of 260 m length and $\tau = 0.07$–0.51; $D_m = 1$–10 mm, $V = 1.0$–4.5 m/s, $V_\perp = 0.3$–1.9 m/s, and $\sigma_I = 0.03$–0.58. The measurements have been performed in 9 snowfalls. One can see from this figure that $A_{0.5}$ in this range of conditions actually does not depend on the correlation time $t_{0.5}$. Its average value equals to 0.16, the maximum value is 0.3, and the minimum value is 0.06. The difference reaches 5 times. We assume that it is caused by the natural variations in D_m and its average value of the snowflake size D_{av}, which we do not measure in the experiment. We assume also that the knowledge of D_{av}, $V_\perp$, and of the gravitational velocity of fall of precipitation particles would allow us to comprehend a behavior of $A_{0.5}$ in the atmospheric precipitation.

2.4. Some characteristics of the NACF

One more peculiarity in $b(t)$ consists in that $b(t)$ has no scales (parts) expressed clearly which are caused by the turbulence and snowflakes. Also as one can see from the presented figures, the function $b(t)$ first quickly falls off with time, and then slowly approaches zero. But, we have no enough reasons to relate this peculiarity in $b(t)$ to two different-scale causes of fluctuations. To answer this question, the direct measurements of the spatial correlation function of intensity fluctuations $B_I(\rho)$ could be useful. We should like to underline that in the spectrum of fluctuations (especially for weak atmospheric precipitation) the turbulent (low-frequency) and hydrometeor (high-frequency) maxima are observed, but between the maxima the spectrum does not fall down to zero.[6] The latter circumstance, seemingly, causes the fact that $b(t)$ has no explicitly manifested scales.

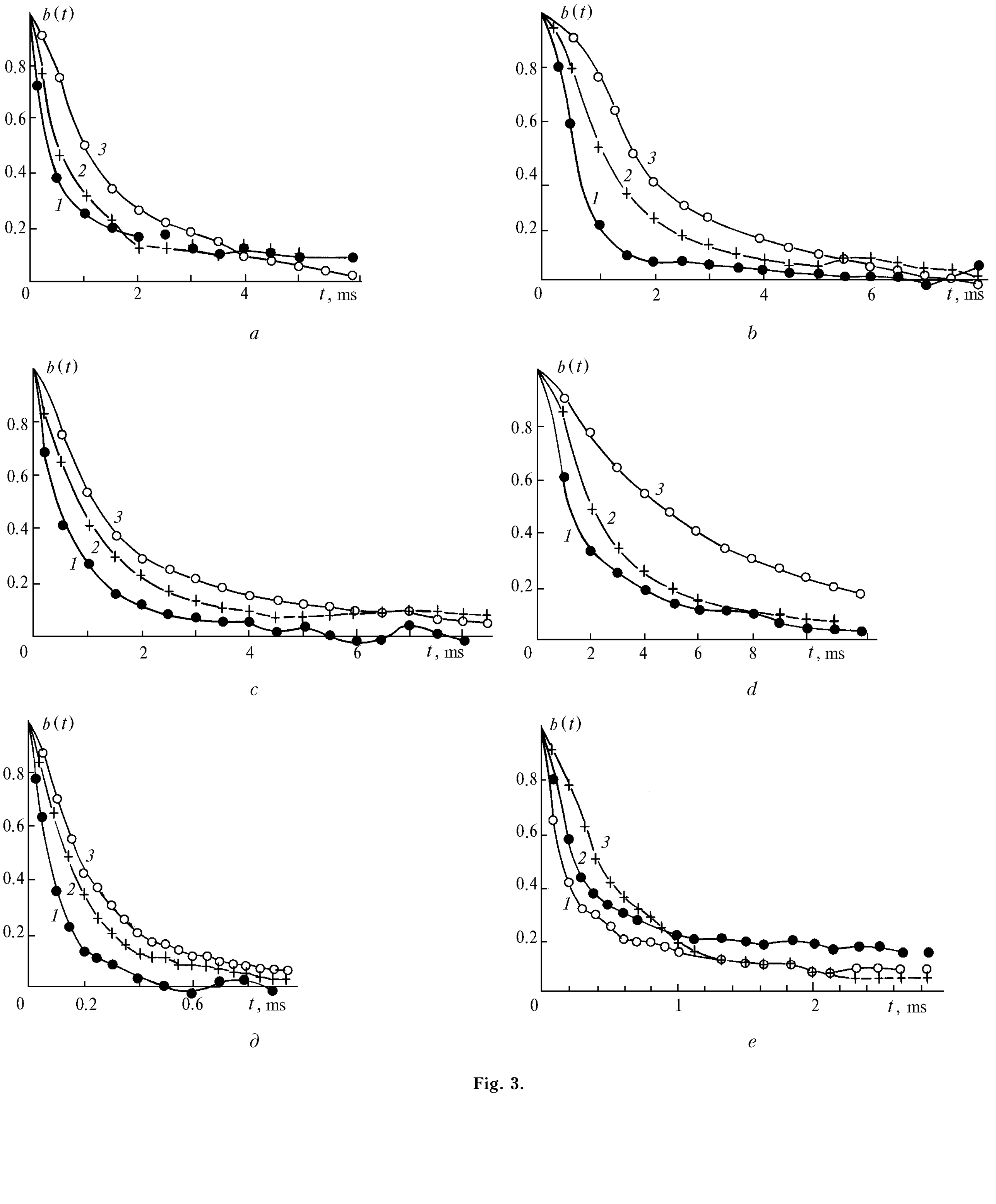

Fig. 3.

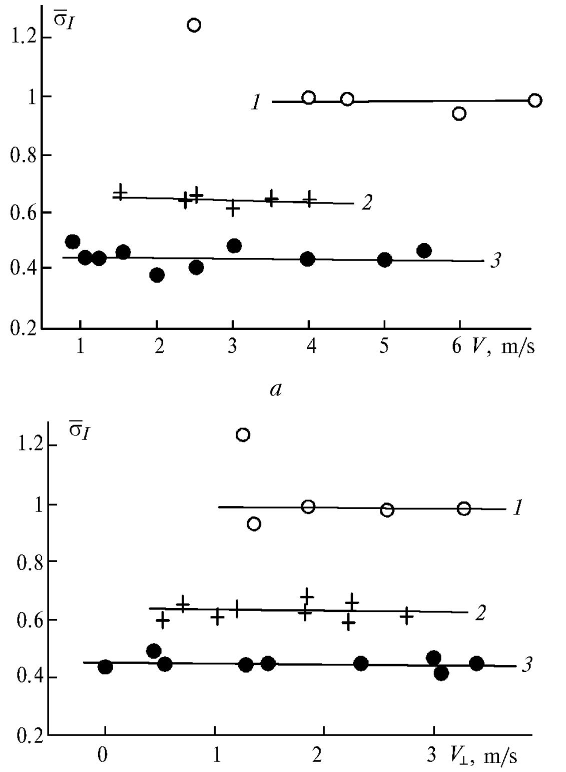

Fig. 4.

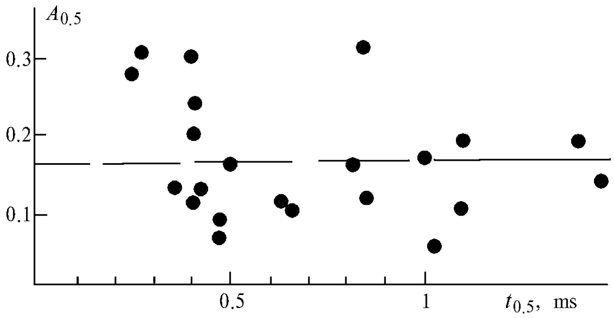

Fig. 5.

The optical depth has an especial importance because it matters essentially[7] in attenuation of radiation. Moreover, it changes to a considerable degree the actual pattern of fluctuations.[8] It is easy to see that we can have the same values of the optical depth for different paths at not identical concentration of snowflakes. Actually, this means that in the given case not identical turbulent conditions will be realized because $\sigma_t^2 \sim L^{11/6}$ under conditions of weak fluctuations, at the same time $\tau \sim L$ (where σ_t^2 is the turbulent contribution to the fluctuations measured experimentally σ_e^2). Equally with this uncertainty during the measurements we can have different D_m and $V_\perp$ which essentially effect $b(t)$.

In connection with these circumstances we performed a comparative analysis of $b(t)$ for various τ but for close values of τ_0, σ_t^2, $V_\perp$, D_m, and equal D_r. As the concentration of particles, the optical depth τ_0 of the 130-m-long path was taken. It was calculated from the data of the visibility meter RDV–3. Estimation of σ_t^2 was performed using the fluctuation spectrum and σ_e^2. We considered that $\sigma_e^2 = \sigma_t^2 + \sigma_h^2$, where σ_h^2 is the hydrometeor contribution to σ_e^2. Atmospheric conditions for which the comparative analysis of $b(t)$ was carried out are very strict for various τ and significantly narrow our opportunities. It was found that we have no enough data for well-founded conclusions. Therefore the effect of τ on $b(t)$ at present remains undetermined even for fixed D_r.

As regards the shape of NACF it varies during the time. Most often NACF falls off linearly with the growth of the delay t at the level 0.5, and sometimes it falls down to the level 0.3. We detect this peculiarity in 150 NACFs from the total 175 analyzed. However, the dependence of NACF on t is not described always by the linear dependence at small t. The approximation of NACF by the linear dependence at $t = 0$ gives sometimes the values of $b(t)$ which exceed unity (but they are below 1.1).

3. Discussion of the results

We begin with the peculiarities in the motion of snowflakes. They have a small velocity of gravitational fall W, which is not more than 2 m/s. At a certain wind velocity V the snowflakes move by the trajectory inclined to the Earth surface at a speed $V_{mv} = \sqrt{W^2 + V^2}$ (Ref. 10, chapter 3). When $W < V$ the velocity of particle motion V_{mv} approximately equals to the wind velocity. Motion of particles of atmospheric precipitation across an optical beam causes a natural change of optical properties of scatterers and their number in the direct beam. From this reason the effect of $V_\perp$ on $b(t)$ appears. The effect of $V_\perp$ on the turbulent spectrum of fluctuations of optical radiation in the atmosphere under condition of clear weather (without precipitation) is well described in Refs. 9 and 11, and, in our opinion, does not require additional explanations.

The effect of D_m on $b(t)$ is obtained for all D_r. To explain this peculiarity, we should take into consideration the following facts. Irrespective of the reasons forming the optical field inhomogeneities in the reception plane, the effect of averaging operation of the receiving device aperture on the value of received signal fluctuations depends on the ratio of the receiver's diameter to the spatial radius of correlation of radiation intensity fluctuations (r_I). The effectiveness of the averaging increases with the growth of this ratio.

In the turbulent atmosphere (without atmospheric precipitation) for a plane wave at $K_s L/k \ll 1$ (where $K_s = 2\pi/l_0$, l_0 is the inner scale of turbulence) the spatial correlation radius r_I has an order of $\sqrt{\lambda L}$ (Ref. 9, §53). Physics of averaging is expounded in the monograph by V.I. Tatarskii. In the case when the telescope diameter significantly exceeds the fluctuation correlation radius $\sqrt{\lambda L}$, the parts of wave front with the opposite signs of fluctuations will be within the diameter. As a result, the total light flux through the objective will fluctuate relatively weaker than for the small (compared with $\sqrt{\lambda L}$) objective (Refs. 9, §53 and 11). In the analyzed experiments the objective diameter plays the role of the diameter ($D_{\rm r}$) of the aperture diaphragm placed in front of a PMT. Physics of averaging of optical radiation by a receiver in the atmospheric precipitation is the same as that for the turbulent atmosphere without precipitation. Therefore, the growth of $D_{\rm r}$ (for close τ, $V_\perp$, and $D_{\rm m}$ values) causes a decrease of the fluctuation level, narrowing of temporal spectrum from the side of high frequencies, and natural increase of the correlation time. It is reflected in Figs. 1 and 2. For the limited spatially beams in the range of weak fluctuations the diffraction size of a beam is the scale of spatial correlation (Ref. 11, §5.1.3). Averaging of fluctuations of a spherical wave over the receiving aperture in the range of weak fluctuations has been considered in Refs. 12 and 13. The effect of inner scale of turbulence on the averaging has been considered in Ref. 14. A comparison of calculations with the experiment was presented in Ref. 14 too. Taking into account the inner scale of turbulence allows us to improve the agreement between the theory and experiment.

The experimental functions of averaging of annular receiving aperture are analyzed in Ref. 15 for the reflection of a spherical wave from a mirror disk and two-dimensional matrix of corner-cube reflectors. The results in Ref. 15 for small apertures (up to 50 mm) are close to the data from Ref. 14. It is considered, that this is connected with the fact that for reflected "quasi-spherical" wave the intensity fluctuations have the spatial correlation radius in the near range, which is larger than at the direct path that is revealed for the use of small apertures. Such peculiarities of r_I are in the turbulent atmosphere without precipitation. In the presence of precipitation, these turbulent peculiarities can be different depending on the time and intensity of atmospheric precipitation.

Now, it is worth saying a few words about possible behavior of r_I in a scattering medium. Every snowfall has its own properties because for optical waves it is essential not only the concentration of particles but their external shape and the inner structure too. They essentially vary in different snowfalls. Moreover, even during the same snowfall the optical properties of particles of atmospheric precipitation change essentially.

In this connection we have analyzed the synchronous measurements of $V(V_\perp)$, $\tau(\tau_0)$, $D_{\rm m}$, and $b(t)$ at the receiving end of the path, but in this case the spatial variations of optical characteristics of atmospheric precipitation along the long path are ignored. Similar difficulties occur when the fluctuations are measured at long paths under clear weather (without precipitation).

Now consider a possible behavior of r_I in a scattering medium. As in Refs. 8, 16, and 17 we divide the field of waves scattered by a single particle of atmospheric precipitation into two components that differ qualitatively from each other:

$$\mathbf{E} = \mathbf{E}_g + \mathbf{E}_n.$$

Here $\mathbf{E}_g$ is the field due to diffraction on the contour of a particle; $\mathbf{E}_n$ is the refracted and reflected field inside a particle. Superposition of the fields $\mathbf{E} = \mathbf{E}_g + \mathbf{E}_n$ is characteristic of the field scattered by an ensemble of atmospheric precipitation particles too. Correlation radius of intensity fluctuations of the refracted field equals to the wavelength,[17] and such fluctuations can not be measured in general schemes of measurement where $D_{\rm r} \gg \lambda$. The situation with the diffraction field is quite different. If all particles of the scattering medium are in the wave zone, i.e., at the distances $r \gg s$ from the radiation receiver, then the diffracted field at a receiver is the superposition of diverging waves and the correlation radius of the intensity fluctuations in accordance with Refs. 8, 16, and 17 is estimated as $r_I \sim d/\tau$ for $\tau > 1$ and $r_I \sim d$ for $\tau < 1$. Here $s = kd^2$, $k = 2\pi/\lambda$, λ is the wavelength, d is the diameter of a particle, τ is the optical depth of the medium. The particles which are in the layer nearby the receiver ($r \ll s$) form shadows in the receiver plane that increases the role of the path layer being adjacent to a receiver in fluctuations. Correlation radius of the intensity fluctuations of the field diffracted on particles from the layer being adjacent is estimated to be equal to the particle diameter.

In the experiment on the long paths the precipitation particles were present both in the near zone and in the far zone of the receiver. But, the importance of the layer of particles adjacent to a receiver is considered as main in forming the fluctuations.[16,17] The thickness of this layer that we roughly estimate depends on the size of particles. For narrow divergent beams, the layer with the thickness $r \sim s$, which is adjacent to a receiver, is important in forming the fluctuations. Complete screening of a beam by the snowflakes will occur in this layer. Hence the dependence of $b(t)$ on $D_{\rm m}$ becomes clear. A decrease in r_I with the growth of τ can be estimated by the corresponding decrease of $t_{0.5}$. From the analyzed data the regular decrease of r_I with the growth of τ is not obtained. It is possible that the small number of data for the large τ ($\tau > 5$) and the errors in determination of $D_{\rm m}$, τ, and $\sigma_{\rm t}^2$ have effected this.

Basic conclusions

The results of analysis of the experimental data allow us to obtain following main characteristic peculiarity in the correlation time ($t_{0.5}$). Under similar atmospheric conditions on D_{m} and $V_{\perp}$, the correlation time $t_{0.5}$ decreases when the receiver diameter decreases. Moreover, it decreases with the growth of $V_{\perp}$ and the decrease of maximum size of the snowflakes that softens the main peculiarity under the atmospheric conditions differing by D_{m} and $V_{\perp}$.

Such a behavior at $t_{0.5}$ is quite an expected one, but it is impossible to consider it as an evident fact.

Acknowledgments

This study was partially funded by the Russian Foundation for Basic Research (Grant No. 99–02–16933).

References

1. A.F. Zhukov and N.A. Vostretsov, Atmos. Oceanic Opt. **9**, No. 6, 670–676 (1996).
2. V.N. Galakhov and R.Sh. Tsvyk, Prib. Tekh. Exp., No. 53, 140–141 (1980).
3. G.Ya. Mirskii, *Electronical Meauserements* (Mir, Moscow, 1986), 439 pp.
4. N.A. Vostretsov and A.F. Zhukov, in: *Abstract of Reports at II Interrepublic Symposium on Atmospheric and Ocean Optics*, Tomsk (1996), P. 1, pp. 133–134.
5. A.F. Zhukov, Atmos. Oceanic Opt. **6**, No. 1, 19–21 (1993).
6. A.G. Borovoi, N.A. Vostretsov, A.F. Zhukov, R.Sh. Tsvyk, and V.P. Yakubov, Atmos. Oceanic Opt. **10**, No. 12, 1012–1013 (1997).
7. M.A. Seagraves, J. Atmos. Sci. **41**, No. 6, 1827–1835 (1984).
8. A.G. Borovoi, N.A. Vostretsov, A.F. Zhukov, B.A. Kargin, and S.M. Prigarin, Atmos. Oceanic Opt. **10**, No. 3, 141–145 (1997).
9. V.I. Tatarskii, *Wave Propagation in a Turbulent Medium*, (McGraw-Hill, New York, 1961), 586 pp.
10. I.V. Litvinov, *Structure of Atmospheric Precipitations* (Gidrometeoizdat, Leningrad, 1974), 154 pp.
11. V.E. Zuev, V.A. Banakh, and V.V. Pokasov, *Optics of Turbulent Atmosphere* (Gidrometeoizdat, Leningrad, 1988), 270 pp.
12. A.I. Kon, Izv. Vyssh. Uchebn. Zaved., Ser. Radiofizika **12**, No. 1, 149–152 (1969).
13. G.E. Homstad, I.W. Strohbehn, R.H. Berger, and I.M.Heneghan, J. Opt. Soc. Am. **64**, No. 2, 162–166 (1974).
14. I.H. Churnside, Appl. Opt. **30**, No. 15, 1982–1994 (1991).
15. G.Ya. Patrushev and O.A. Rubtsova, Atmos. Oceanic Opt. **6**, No. 11, 798–801 (1993).
16. A.G. Borovoi, Izv. Vyssh. Uchebn. Zaved., Ser. Radiofizika **25**, No. 4, 391–400 (1982).
17. A.G. Borovoi, "*Multiple scattering of optical waves in media with discrete scatterers*," Author's Abstract of Doct. Phys.-Math. Sci. Dissert., Tomsk (1984), 36 pp.